SC/64/AWMP1

Molecular insights to historical demography in Bowhead whales

Phillips, C. D.[Ω], J. I. Hoffman†, J. C. George[τ], R. S. Suydam[τ], R. M. Huebinger[α], J. C. Patton[§] and J. W. Bickham[§]

[Ω]Department of Biological Sciences, Texas Tech University, Lubbock, Texas, USA. †Department of Animal Behaviour, University of Bielefeld, Bielefeld, North Rhine-Westphalia, Germany. [τ]North Slope Borough, Department of Wildlife Management, Barrow, Alaska, USA. [α]University of Texas Southwestern Medical Center, 5323 Harry Hines Blvd, Dallas, TX, USA. [§]Department of Forestry and Natural Resources, Purdue University, West Lafayette, Indiana, USA.

Abstract

Bowhead whales are characterized by relatively high genetic diversity, great longevity, long generation time, and are known to have experienced a dramatic depletion in population size as a result of commercial whaling in the late 19th and early 20th Centuries. The Bering-Chukchi-Beaufort Seas stock is thought to have been reduced to as few as 1,000 individuals as a result of this occurrence. Because this population is managed to support the subsistence harvest of Alaskan and Chukotkan native communities, estimating ancestral population sizes and the degree to which the population was reduced by commercial whaling has both practical significance in the determination of population growth rates, as well as being of intrinsic interest to understanding historical demography. In this study we investigated the demographic history of this population using a variety of analytical methods, including approximate Bayesian computation, extended Bayesian skyline analysis, in addition to many classical bottleneck and demographic tests. The results of approximate Bayesian computations support a pre-depletion ancestral population size of 10,000 to 20,000 individuals; however, uncertainty over mutation rate limited the precision of this estimation using this analytical approach. In addition, signal for a historical population expansion having begun approximately 75,000 years before present was supported by multiple analyses. A subsequent, non-anthropogenically driven, population reduction, that ensued about 15,000 years ago, was also detected. No genetic signature for the recent population depletion was recovered through any analysis incorporating realistic mutation assumptions. Conclusions are that while bowhead whales have a dynamic demographic history, the reduction in population size caused by commercial whaling was of insufficient magnitude to contribute to this genetic history. The biological basis for this is that the bottleneck was of short duration in relation to the long generation time of the bowhead. The latter served as a buffer to minimize erosion of variability through genetic drift.

Introduction

Inference on the demographic history of species is an important component to understanding how evolutionary processes shape contemporary genetic variation. Applied to species with a history of an anthropogenic demographic disturbance, such studies help to explain how the combination of life history and disturbance parameters interact to result in species-specific genetic responses to demographic change. Human induced population declines are often well documented in terms of duration and severity, and can therefore lend valuable insight into evolutionary processes.

Marine mammals, especially whales, are particularly interesting in the context of exploring demographic history because many are characterized by a recent history involving drastic population reductions as a result of unregulated commercial harvest which has been well documented in many instances. In contrast, their more ancient past is less well known than for many terrestrial species due in part by the fact that geological events such as ice ages and continental drift have less direct impact on their history. Whales have several remarkable life history characteristics, among which is a long generation time, a life history parameter that potentially protects them from the erosion of genetic diversity by drift when a bottleneck is of short duration.

Furthermore, general public interest and continued aboriginal, scientific, and commercial harvest of some whale species provides increasing relevance to demographic investigations in whales.

Several analytical approaches have been developed to investigate historical demographic changes using genetic data. Some of these, explicitly defined as 'bottleneck analyses', exploit expected changes in allele frequency, heterozygosity, or allele size distributions resulting from genetic bottlenecks. Probably the most well-known and widely applied is the heterozygosity excess test developed by Luikart et al. (1998) that detects signal for the expected transient excess of heterozygosity that can arise during genetic bottlenecks. A very different approach that can be applied to understanding demographic change using microsatellite and/or sequence data is approximate Bayesian computation (Beaumont et al. 2002). This method employs coalescent based simulations of alternative demographic scenarios, which are compared to the observed data through summary statistics. Simulated data producing summary statistics most similar to the observed are retained to estimate the posterior distributions of demographic parameters, such as the timing of events, associated effective population sizes (N_e) and marker mutation rates (μ). This increasingly popular approach has recently been shown to be powerful for detecting bottlenecks in species with exceptionally well characterised recent demographic histories (e.g. Chan et al. 2006, Hoffman et al. 2011).

Other tests capable of detecting demographic change, explicitly developed for sequence data, include commonly applied statistics such as Tajima's *D* (Tajima 1989), Fu's F_S (Fu 1997), and the raggedness index (Harpending 1994). These methods rely on the comparison of nucleotide diversity and segregating sites (as θ estimators), allele diversity, and the frequency distribution of pairwise distances, respectively. The first two of these methods are classically defined as neutrality tests, although demographic changes are also readily detected, and the latter can be influenced by factors other than demography (i.e. selection or migration). Finally, Bayesian skyline plotting, a method that reconstructs demography over time using the coalescent and directly from a sequence alignment and the estimated phylogeny, has evolved through a progression of statistical developments (Drummond & Rambaut 2007). This method is unique in its ability to provide a continuous demographic reconstruction over time, and without *a priori* demographic assumptions. Although this brief summary of different methods emphasizes their differences, all methods share the commonality of exploiting the fact that demographic change alters the patterns of variation observed in genetic data sets.

The bowhead whale, *Balaena mysticetus*, is the second largest species of whale, has an estimated generation time of greater than 50 years (Taylor et al. 2007), and may routinely live > 100 years, with maximum age possibly in excess of 200 years (George et al. 1999). This species is an important food source for some native communities in Alaska and Chukotka, who enact an annual sustainable harvest, the quota for which is provided by the International Whaling Commission. There are four recognized populations of *B. mysticetus*, termed stocks that are characterized by differences in geographic distribution, migration patterns and demographic trends, but display only relatively low levels of genetic divergence. Of these four stocks, the Bering-Chukchi-Beaufort Seas stock (BCB) is the largest and most intensely harvested. Unregulated commercial whaling from 1848-1914 resulted in an estimated 93% population reduction of the BCB, reducing the population to around 1,000 individuals (Rooney et al. 2001; Punt 2006). George et al. (2004) estimated the census size of the BCB in 2001 to be 8,100-13,500 (mean 10,470) and increasing at 3.4% annually. Currently the BCB stock is considered to comprise approximately 13,000 individuals.

Clues about ancient demographic phenomena come from Rooney et al. (1999), who under specific microsatellite mutation assumptions, reported signal for a population expansion estimated to have occurred 8,500 years before present (ybp) following the M'Clintock Channel Sea Ice Plug formation that would have isolated the BCB from the eastern Canadian Arctic stock. Presently a larger microsatellite dataset exists for this study based on 22 microsatellite loci derived from bowhead sequences (Huebinger et al., 2008) which were found to perform better than the 20 loci used by Rooney et al. (1999) which included markers derived from bowheads as well as a variety of nont-target species and a larger sample size (Givens et al., 2010). We also greatly expand the on previous bowhead mtDNA studies (Rooney et al., 2001; LeDuc et al., 2008) by

including sequence data from 3 mitochondrial gene regions instead of just the control region as in the previous studies. In this study we test demographic hypotheses posed in previous studies including the recent depletion caused by commercial whaling, and the ancient population expansion hypothesized by Rooney et al. (1999), and we explore evidence of previously unreported demographic events.

Materials and Methods

Tissue sample collection and DNA extraction
Tissues were collected from 324 whales from the Bering-Chukchi-Beaufort Seas (BCB) stock of bowhead whales. All specimens were analyzed for 22 microsatellite loci and 168 were analyzed for 3 mitochondrial gene regions. The majority of the samples were obtained via necropsy sampling of whales that were part of Alaskan aboriginal subsistence harvests. Six tissue samples were obtained from remote biopsy darting. Table 1 presents sampling locations (8 Alaskan villages) and number of samples collected from each location. Tissues and DNA samples were stored at -80ºC. DNA was extracted from skin slices or biopsy plugs using the GenElute mammalian genomic DNA purification kit (Sigma-Aldrich; St. Louis, MO)

Microsatellite genotyping
The extracted genomic DNA was quantified by gel electrophoresis on 1.0% agarose gels and visualized on an Eagle Eye II (Strategene, LaJolla, California). The genomic DNA extract was used as a template to amplify 22 microsatellite loci as detailed in Huebinger et al., (2008). The loci are described in Table 2. The PCR reactions consisted of 50 ng of genomic DNA, 0.5 units of *Taq* polymerase, 1.5 mM $MgCl_2$, 200 µM each dNTP , 12.5 pmol forward (fluorescent labeled)primer and 12.5 pmol reverse primer. The 15µL reactions were cycled 36 times at the following temperatures: 95°C for 20 seconds to denature, variable temperature (primer dependent, Table 2) for 15 seconds to anneal, and 72°C for 30 seconds for extension. The amplification products were visualized on an Eagle Eye II (Strategene) for a rough quantification. Allele sizes were determined by fragment separation on an ABI3100 DNA Analyzer (Applied Biosystems, Inc; Foster City, CA). . Fragment lengths were assigned by the GeneMapper software program (Applied Biosystems, Inc.) using GeneScan-400 [ROX] size standard. Samples that produced poor quality chromatograms or failed to amplify were reanalyzed. A thorough description of the microsatellite dataset was previously reported by Givens et al. (2010).

Mitochondrial DNA sequencing
Sequences from three mitochondrial gene regions, HVRI (397 base pairs), Cytb (1140 base pairs), and ND1 (957 base pairs) were obtained. Detailed methods are described in LeDuc et al. (2008) for HVRI and Phillips et al. (2011) for the two protein coding genes.

Data analyses
Tests for deviation from Hardy-Weinberg equilibrium and for linkage disequilibrium were implemented using GENEPOP v. 3.1d (Raymond and Rousset 1995). Bonferroni adjustments (Hochberg 1988) with an α level of $P \leq 0.05$ were carried out on all tabulated results. GENEPOP was also used to determine expected and observed heterozygosity (H_E and H_O, respectively). Null allele frequencies were calculated following Chakraborty (1998) using the program Micro-checker (Van Oosterhout et al. 2004).

Classical microsatellite-based bottleneck tests
To test for evidence of a recent demographic decline or expansion, we analysed the microsatellite data for deviations from expected heterozygosity at mutation-drift equilibrium within the program BOTTLENECK v 1.2.02 (Piry et al. 1999). Six different mutation models were evaluated: the strict Stepwise Mutation Model (SMM, Kimura and Ohta 1978), the Infinite Alleles Model (IAM, Kimura and Crow 1964) and four intermediate Two-Phase Models (TPMs) with 1%, 5%, 10% and 30% IAM mutations respectively. For each mutational model, the heterozygosity of each locus expected at equilibrium given the observed number of alleles (H_{eq} was determined using 10,000 simulations and then compared against observed heterozygosity

(H_e). We then recorded the number of loci for which H_e was greater than H_{eq} and smaller than H_{eq}, and determined whether the overall set of deviations was statistically significant using sign, standardized differences and Wilcoxon signed ranks tests. Finally, BOTTLENECK was also used to generate a qualitative descriptor of whether the observed allele frequencies at each locus deviate from the L-shaped distribution expected under mutation-drift equilibrium Luikart at al. (1998).

Classical sequence-based demographic tests

Concatenation of the mitochondrial gene regions resulted in a 2494 base pair sequence. One-hundred-sixty-eight individuals sequenced for all three gene regions were included for analyses (Table 1). Arlequin version 3.5.1.2 (Excoffier et al. 2005) was used to calculate multiple statistics. Tajima's *D*, useful for detecting departures from population equilibrium, selection, and rate heterogeneity, was calculated based on uncorrected pairwise comparisons. Significance was assessed by randomly generating samples under the hypothesis of neutrality and observing the proportion of simulated values less than or equal to the observed (Hudson 1990; Excoffier et al. 2005). Fu's F_S, a test statistic that is sensitive to departure from population equilibrium, was also calculated. While Tajima's *D* relies on the comparison of estimators of θ, Fu's F_S relies on comparison to the observed allelic abundance to that obtained through simulation under neutrality. Similar to that implemented for Tajima's *D*, significance for Fu's F_s is obtained by the proportion of times simulated F_S values are equal to or smaller than the observed. A mismatch distribution and the associated raggedness index were also calculated. The mismatch distribution was based on uncorrected pairwise differences, and significance was based on the sum of squared deviations of the observed and expected mismatches that were obtained by generating 1000 random samples according to the estimated demography. Following an observed non-significance raggedness index, the timing of the postulated demographic expansion was estimated assuming a generation time of 52 years (Taylor et al. 2007), an overall mutation rate (μ) of 1.18%/million years (obtained by averaging independent rate estimates for each gene region obtained through Bayesian demographic reconstructions, see below), and following the algorithms of Watterson (1975), Rogers (1995), and Schneider and Excoffier (1999) for estimating τ ($\tau = 2\mu t$, where t is the time to demographic expansion).

Extended Bayesian skyline plot

To explore signal contained in the mitochondrial data set for demographic change over time, an extended Bayesian skyline plot (EBSP) was calculated. Bayesian skyline plots are based on the coalescent and use the estimated phylogeny to reconstruct demographic change without prior assumptions on the timing of events (Drummond & Rambaut 2007). The EBSP is an implementation of the Bayesian skyline plot that incorporates multi-locus information in the demographic reconstruction. As discussed by Heled and Drummond (2008), multi-locus perspectives about demographics empower reconstructions. Although, separate regions of the mitochondrial genome can be accurately considered as a single locus, ESBP was implemented here to allow separate phylogenetic reconstructions for each locus separately. For analysis, a mutation rate for HVRI was defined as 2.8%/million years. This value was obtained following the methods of Alter and Palumbi (2009), in which the synonymous rate at linked coding regions are used to calibrate the HVRI rate. ND1 and Cytb were assigned relaxed molecular clocks (as deemed appropriate through clock testing in MEGA version 5; Tamura et al. 2007) and their rates were estimated from the data in relation to that assumed for HVRI. Fifty-million MCMC sets were conducted, with sampling every 1000 iterations. Effective samplings of prior and posterior tree distributions were confirmed in Tracer (Rambaut and Drummond 2007). The last 10,000 iterations of simulations were retained for ESBP analysis.

Approximate Bayesian computation

Approximate Bayesian computation, originally introduced by Beaumont et al. (2002), was implemented in DIYABC v1 (Cornuet *et al.* 2008; Cornuet *et al.* 2010). Demographic models were defined to capture genetic signal present in the data that has been suggested by previous studies based on both genetic and census data. These findings served as *a priori* demographic information around which models tested through approximate Bayesian computation were developed. Generation time, an important parameter for demographic reconstruction, was defined as 52 years, as reported by Taylor et al. (2007). A 1:1 sex ratio was implemented

based on data from Nerini et al. (1984); Heide-Jørgensen et al. (2010) and J. C. George (unpublished harvest data). Two demographic models were simulated for comparison. These models were defined by identical priors on time to account for historic events. Specifically, time priors employed represented a demographic event uniformly distributed between one and six generations ago (encompassing the timing of the known period of unregulated whaling), and two additional time priors uniformly distributed with equivalent prior distributions between 7 and 357 generations ago (population expansion population size, and ancestral population size). The upper bound on these time parameters extended to 18,500 ybp, liberally surrounded the timing of the postulated population expansion of Rooney et al. 1999). Prior distributions on N_e associated with each time were defined by uniform distributions between 1 and 20,000, with the exception of the bottleneck model, which incorporated a uniform N_e prior of 1-2,000 associated with the initial time prior (1-6 generations). The purpose of confining the prior distribution on N_e at this time period was to enforce N_e values during this interval to that expected given the census population size at that time. As such, demographic models were identical with the exception of N_e associated with the bottleneck time prior. N_e parameters are subsequently referred to as $N_{e(contemporary)}$, $N_{e(bottleneck)}$, $N_{e(historicA)}$, $N_{e(historicB)}$, with the latter two being the N_e parameters associated with identical time priors. Microsatellite μ was defined as the generalized stepwise mutation model (Estoup *et al.* 2002) with a mean rate uniformly distributed between 1.00×10^{-5} and 1.00×10^{-3} substitutions/generation. Although the lower bound on this prior distribution is lower than that generally assumed for microsatellites, previous studies have indicated a reduced evolutionary rate in whales as compared to that usually observed in mammals (Alter and Palumbi 2009). For mitochondrial sequences, the employed model of evolution determined through model testing in MEGA 5 (Tamura et al. 2007) was HKY + I (0.5) + G (0.05). This substitution rate was uniformly distributed between 1×10^{-7} and 1×10^{-8} substitutions/site/generation.

Sensitivity to prior assumptions in approximate Bayesian computation inference has previously been acknowledged by other authors (Chan et al. 2006; Hoffman et al. 2011). To explore the influence of prior assumptions about N_e on posterior estimates, additional simulations were performed incorporating a range of prior bounds on N_e. Subsequent simulations were performed in which the N_e parameters originally defined between one and 20,000 were confined to an upper bound of 10,000 (a biologically reasonable upper bound given estimates of ancestral census size), or extended to 50,000, and then to 100,000 in final simulations. Although these latter prior bounds could be interpreted as overly generous given the census population size assumptions derived from the above cited studies, separate studies by Roman and Palumbi (2003) reported considerably larger N_e estimates for several whale species than is generally discussed for *B. mysticetus*. Comparative analysis of all sets of simulations allowed for a diagnosis of how the availability of biological information about N_e (and prior assumptions) influences posterior biological inferences. Initial simulations showed that while simulated microsatellite data fit the observed data reasonably well, simulated mitochondrial data were a poor fit for the observed data (this was assessed by ranking the observed summary statistics against the simulated; Cornuet et al. 2010). Hence the data are not shown and this was not explored further. Additional simulations exploring ranges of N_e assumptions focused on the microsatellite portion of the data set. Alternative explorations of the mitochondrial data were performed using the alternative methodologies described above.

One million simulated datasets were generated for each demographic model. Heterozygosity and mean number of alleles were the computed summary statistics for observed and simulated data sets. These summary statistics were selected because they are known to be influenced by changes in effective population size (Luikart et al. 1998). Model comparisons implemented the local linear regression method introduced by Beaumont et al. (2002). Type I and II error rates in model selection were calculated by simulating 500 data sets under the parameters of each model and assuming the given model was the correct model. From the best supported model ten thousand datasets (1% of total simulations for that model) with the smallest Euclidean distances from the observed were retained to build posterior parameter distributions, which were smooth weighted using the Locfit function within R version 2.9.1 (R Development Team 2005).

Results

Three-hundred-twenty-four individuals genotyped at 22 microsatellite loci were used in the analyses; 305 of these were previously reported in Givens et al. (2010). Moderate to high levels of genetic variability were found, with each locus yielding between six and 28 alleles (mean = 15.7, Table 2) and expected heterozygosity ranging from 0.566 to 0.938 (mean = 0.808). Weakly significant deviations from Hardy–Weinberg equilibrium were detected at four loci (Table 2), but none of these remained significant following table-wide Bonferroni correction for multiple statistical tests (Hochberg 1988). Similarly, no evidence was found for null alleles being present at high frequencies in any of the loci. Tests for linkage disequilibrium yielded 19 significant P-values ($P < 0.05$) out of 231 pairwise comparisons, only one of which remained significant following Bonferroni correction (loci Bmy10 and Bmy26).

Classical sequence-based demographic tests

Both Tajima's *D and* Fu's $F_{S\ were}$ negative and statistically significant (Tajima's $D = -1.4$, $P < 0.05$; Fu's $F_{S\ =}$ -24.3, $P < 0.0001$).The mismatch distribution was unimodal (data not shown) with a raggedness index of 0.003 (the probability that simulated raggedness was greater than or equal to the observed raggedness was 0.89).. Average μ for the concatenated mitochondrial gene regions was estimated at 1.18 %/million years, τ was estimated at 4.34. Following a generation time of 52 years (Taylor et al. 2007), the estimated time to the demographic expansion was calculated at 75,296 ybp.

Extended Bayesian skyline plot

Survey of effective sampling of values in TRACER disclosed values of greater than 200 for all parameters, indicating sufficiently deep sampling (Drummond & Rambaut 2007). Posterior estimates of mutation rates for HVRI, Cytb, and ND1 were calculated at 2.52%, 0.58% and, 0.49%/my, respectively. Reconstructions indicated a demographic history involving a few major episodes of population increase and decline. The demographic reconstruction included an increase in N_{ef} estimated to have begun between 50,000 and 75,000 ybp that continued until about 15,000 ybp, which was followed by a population reduction over subsequent generations (Figure 1). From this reconstruction, current N_{ef} was estimated at a median value of 20,000. Examination of the mean value estimated over the most contemporary times suggested mtDNA signal for a recent increase in N_{ef} over the past few millennia; however, the 95% highest posterior densities disclosed increased uncertainty during this time.

Classical microsatellite-based bottleneck tests

Analysis of the microsatellite dataset within the program BOTTLENECK yielded virtually identical results regardless of whether the full dataset was used or the analysis was restricted to the 18 loci in HWE (Table 3). There was also strong consistency among *P*-values obtained from the sign, standardized differences and Wilcoxon tests. However, the results were highly dependent on the mutational model specified, with a significant excess of heterozygosity being detected under the IAM but a significant deficiency of heterozygosity being found under the SMM. Similarly, the intermediate TPM models indicated a significant excess of heterozygosity when strongly influenced by the IAM (e.g. the TPM70 model) and a significant deficiency of heterozygosity when mutations were predominantly SMM (e.g. the TPM99 and TPM95 models).

Approximate Bayesian computation

Comparison of the initial demographic models indicated the model not enforcing a recent N_e reduction produced simulated data sets yielding summary statistics most similar to the observed. This model received a posterior probability of 0.85, while the model enforcing a genetic bottleneck yielded a posterior probability of 0.15. Type I and Type II error rates for the selection of the best supported model were 0.28 and 0.3, respectively. This model was described by an ancient N_e with a median value of 8,980 (very similar values were obtained for both $N_{e(historicA)}$ and $N_{e(historicB)}$; Table 4). No resolution was recovered for posterior estimates for the times associated with these N_e estimates (data not shown because posterior distributions were flat).

Similarly, the whaling period time prior, it's associated $N_{e(bottleneck)}$, as well as $N_{e(contemporary)}$ all returned flat, or nearly flat, distributions.

Subsequent simulations evoking a range of prior bounds on N_e at all time periods always supported the same demographic model that was supported in initial simulations. However, comparison of posterior estimates of parameters across simulations disclosed sensitivity of prior assumptions on N_e to both the posterior estimates of N_e and μ. Specifically, broader prior assumptions on N_e yielded larger posterior estimates for ancestral N_e, yet smaller posterior estimates for average μ. The posterior distributions of time and N_e parameters from all simulations are available as joint plots in Figure 2 and are listed in Table 4.

Discussion

Few studies have used genetic data to explore historical demographic phenomena over multiple timescales and using a variety of contrasting but complimentary approaches. Here, we used a large dataset of 22 highly polymorphic microsatellite loci and 2,494 bp of mtDNA to elucidate the demographic history of an anthropogenically exploited whale species over the past ~200,000 years. Classical bottleneck and BSP reveal support for a demographic expansion around 75,000 years ago, but we found no evidence of a recent decline in Ne concurrent with the recent history of human exploitation.

Known history of the species

As with many similar species, understanding the demographic history, both recent and more ancient, may have important implications for contemporary management. An annual harvest quota for the Alaskan and Russian aboriginal hunt is provided by the International Whaling Commission using the method of the Aboriginal Whaling Management Procedure (AWMP). Following the AWMP, the existing *B. mysticetus* assessment is driven by the past catch series, the current estimate of abundance in absolute terms, and the current rate of population increase. The current population growth rate is estimated to be 3.4% (George et al. 2004); however, the long term growth rate over the past century is dependent upon the size of the population at its nadir. Taken together and under the conventional population model assumption of compensatory dynamics (the larger the population, the lower the per-capita growth rate), there is indication that the population was very small at the end of the 19th century (D. Butterworth, pers. comm.). However, there is no direct evidence that can provide an abundance estimate during the years of high depletion.

Evidence for historical population expansion

Analysis of 2,494 base pairs from 3 genes of the mitochondrial genome yielded similar results in which Tajima's *D* and Fu's F_S were both found to be significantly negative, both of which are compatible with a history of population expansion. Furthermore, the observed unimodal mismatch distribution not only corroborated these results, but also provided an estimated time of expansion to roughly 75,000 ybp. A previous analysis of the mitochondrial control region by Rooney et al. (2001) also discussed the possibility of a population expansion. These authors constructed lineage through time plots, which can provide a relative demographic reconstruction (time is relative to the phylogeny, not in years), and estimated the coalescence time of bowheads whales. From this analysis these authors rejected the hypothesis of Rooney et al. (1999), in which the M'Clintock Channel Sea Ice Plug formation, which occurred approximately 8,500 years ago, was implicated in a postulated population expansion. Rather, these authors estimated the coalescence time of bowhead whales to approximately 270,000 ybp and assumed that mitochondrial coalescence forward in time was directly followed by population expansion that is only now beginning to wane. In the present study, both the mismatch distribution and the EBSP support a population expansion around 75,000 years ago. In the current study we did not reject the hypothesis of Rooney et al. 1999 *a priori*. Furthermore, when the analysis performed by Rooney et al. (2001) was conducted the estimated current population growth rate of 3.4% annual (George et al. 2004) was not available, and would likely influenced these author's interpretation of a population expansion ensuing for 270,000 years.

The EBSP was useful for providing improved resolution on the demographic history of N_{ef}. Part of the results of this analysis was in agreement with the mismatch distribution; a population increase was recovered through ESBP that was also estimated to have begun about 75,000 ybp and peaked at around 25k ybp (Figure 1). Putatively, this historic event defined many aspects of the patterns of genetic variance observed in the BCB, and is likely the source of the population expansion signal obtained from all other analytical approaches discussed above. However, the EBSP also described a subsequent population reduction, estimated to have taken place over the past 15,000 years. This population reduction is placed within a time period before to the period of known anthropogenic reduction in the 19th and 20th centuries. Because of this, the remaining possibilities to explain this observation are effects of natural biological cycles associated with carrying capacity and/or environmental change.

Evaluation of a bottleneck scenario

Initial testing applied the heterozygosity excess test under a range of mutation model definitions. Observations were that signal for a genetic bottleneck was only observable under the IAM model. Given that the IAM is unrealistic for most 'real' microsatellites (Di Rienzo et al. 1994) and that a TPM model comprising ~5% IAM mutations is more likely (Piry et al. 1999), analyses were actually consistent with a population having undergone a population expansion. Moreover, a shift in the allele frequency distribution from an L-shaped distribution was not observed, suggesting that the population was not recently bottlenecked. Although these results were consisted with previous analyses (Rooney et al. 1999, Givens et al. 2010), they are not in line with what is known about stock depletion through parts of the 19th and 20th centuries suggesting that the bottleneck was not of great enough duration relative to the long generation time of the bowhead to leave a clear signal of heterozygosity excess.

The implementation of approximate Bayesian computation in this study was used to evaluate whether a genetic signature for the known population reduction was in fact present in the data, yet unrecoverable using a variety of alternative statistical assessments. Results of the ABC analysis were in agreement with the classical bottleneck tests. Given that the compared demographic models only differed in the prior constraint on $N_{e(bottleneck)}$, and that Type I and II error were both estimated at approximately 30%, this indicates that a population model involving a recent N_e reduction is not likely to be compatible with the observed data. Furthermore, the ABC analysis showed no support for a population expansion ~8,500 ybp (Rooney et al. 1999), reflected in the flat distributions of time posteriors associated with $N_{e(historicA)}$ and $N_{e(historicB)}$, and lack of signal for N_e during the past 300 years ($N_{e(contemporary)}$ and $N_{e(bottleneck)}$). This is not to say there is lack of signal for estimating effective population size in *B. mysticetus*; rather, that a wide range of N_e values over this time period in conjunction with estimated historic N_e values produce summary statistics similar to that observed in the BCB. In other words, any range of plausible N_e values (range of population sizes) over the past 300 years is not sufficient to drive genetic signal. This is a reflection of the relationship between bottleneck duration, generation time, μ and the design of approximate Bayesian computation (see below).

An additional finding stemming from the approximate Bayesian computation analysis was the importance of prior assumptions on posterior estimations, and hence, biological interpretations. Through a series of simulations that evoked differing degrees of constraint on N_e values, it was found that level of constraint applied was reflected in the posterior estimates. Specifically, tighter and lower prior assumptions on N_e yielded lower point estimates for this parameter. In addition, the posterior estimate of μ was found to be inversely proportional to N_e. This observation is an artefact (for lack of a better word) of approximate Bayesian computation. Because the statistical method relies on disclosing combinations of parameter values that lead to data sets producing summary statistics similar to the observed, parameters such and N_e and μ can take on antagonistic properties. In the case of *B. mysticetus* (or any species of management concern and with a tendency for small effective populations sizes), these assumptions can have influence on biological interpretations. Because *a priori* information about N_e in bowhead whales and μ for whales is available, results obtained from some of the simulations can likely be excluded. For example, although posterior estimates for historic N_e (5,700) stemming from simulations evoking a 1-10,000 N_e prior could be considered

biologically plausible, a rather large value of μ was required, and is not likely given the findings of Alter and Palumbi (2009), in which a generally lower rate of molecular evolution was observed in whales. The alternative scenario was observed in simulations providing a N_e prior of 1-100,000. As such, the real value of historic N_e likely lies within the estimates provided by the simulations with N_e priors of 1-20,000 and 1-50,000, which yielded mean estimates for historic N_e of 10,000 and 20,000 respectively. These results indicate that the ability to make a more exact estimate of historic N_e within this range would require a firm assumption on μ.

To better understand the basis for the results of all analyses, we conducted a set of *post hoc* simulations using SPAms (Parreira et al. 2009). The major parameters of the simulations involved μ (assumed as 1×10^{-4}), ancestral N_e, contemporary N_e, and generation since the change in population size. Multiple sets of simulations were performed to represent a range of combinations of the latter three parameters. Each demographic simulation was iterated 1000 times, expected heterozygosity was calculated, and then plotted using SAS version 9.1 (SAS Institute Inc.). The details of this simulation are listed in the caption of Figure 3. As illustrated, the simulation potentially most similar to that actually experienced by *B. mysticetus* according to all available information resulted in no loss of genetic variability. In fact, combinations of smaller contemporary N_e and increased bottleneck duration (having occurred much further in the past) were required to begin to produce a measurable impact of population reduction. This may be partly due to the relationship between generation time and bottleneck duration and that genetic drift increases with decreasing population size. The estimated 52 year generation time of bowhead whales translates to only a transient demographic bottleneck by the harvest-induced depletion. Similar trends in other long-live species have been previously documented (i.e. white-tailed eagles, Hailer et al. (2006), and in the copper redhorse, Lippé et al. (2006)). By comparison, however, Hoffman et al. (2011) recently detected signature for a genetic bottleneck in the Antarctic fur seal, a species with a larger anthropogenic N_e reduction (a reduction from 1.5 million down to perhaps 30 individuals) and decreased N_e (nine years) relative to bowhead whales, yet having occurred at about the same time (mid to late 19th and early 20th centuries). Combined, the finding of this study, previous demographic studies on *B. mysticetus*, and those in other species, all indicate that the characteristic long generation time of bowhead whales has served as a protective buffer to hunting induced population decline.

Conclusions

This paper used multiple analytical methods to explore the demographic history of bowhead whales using expanded datasets for both mtDNA and microsatellites. The results consistently show evidence of an ancient population expansion beginning 75,000 ybp and peaking about 25,000 ybp, and a population decline about 15,000 ybp. No evidence for a significant genetic bottleneck was found associated with the recent population depletion caused by commercial whaling. It is concluded that the great generation time of this species served as a buffer to prevent the loss of genetic variation during the short duration of the bottleneck sufficient to be detected by current methods.

Acknowledgements

We thank the Alaska Eskimo Whaling Commission (AEWC) and the Barrow Whaling Captains' Association for their confidence, guidance and support of our research. We gratefully acknowledge funding provided by the North Slope Borough Department of Wildlife Management and National Oceanic and Atmospheric Administration (through the AEWC). D. Butterworth and G. Givens provided helpful comments during the development of this paper.

References

Alter SE, Palumbi SR (2009) Comparing evolutionary patterns of variability in the mitochondrial control region and cytochrome *b* in three species of baleen whales. *Journal of Molecular Evolution*, 68, 97-111.

Beaumont MA, Zhang W, Balding DJ (2002) Approximate Bayesian Computation in Population Genetics. *Genetics* 162, 2025-2035.

Chakraborty R (1988) Analysis of genetic structure of a population and its associated statistical problems. *Sankhya-the Indian Journal of Statistics Series B*, 50, 327-349.

Chan YL, Anderson CNK, Hadley EA (2006) Bayesian estimation of the timing and severity of a population bottleneck from ancient DNA. PLoS *Genetics*, 2, e59.

Cornuet JM, Ravign V, Estoup A (2010) Inference on population history and model checking using DNA sequence and microsatellite data with the software DIYABC (v1.0). *BMC Bioinformatics,* 11, 401.

Cornuet JM, Santo F, Beaumont MA, et al. (2008) Inferring population history with DIYABC: a user-friendly approach to Approximate Bayesian Computations. *Bioinformatics*, 2713-2719.

Di Rienzo A, Peterson AC, Garza JC, Valdes AM, Slatkin M (1994) Mutational processes of simple sequence repeat loci in human populations. *Proceedings of the National Academy of Sciences of the United States of America*, 91, 3166-3170.

Drummond AJ, Rambaut A (2007) BEAST: Bayesian evolutionary analysis by sampling trees. *BMC Evolutionary Biology*, 7, 214.

Estoup A, Jarne P, Cornuet JM (2002) Homoplasy and mutation model at microsatellite loci and their consequences for population genetics analysis. *Molecular Ecology*, 11, 1591-1604.

Excoffier, L. G. Laval, and S. Schneider (2005) Arlequin ver. 3.0: An integrated software package for population genetics data analysis. *Evolutionary Bioinformatics Online*, 1, 47-50.

Fu YX 1997 Statistical tests of neutrality of mutations against population growth, hitchhiking and background selection. *Genetics*, 147, 915-925.

George JC, Follman E, Zeh J, Sousa M, Tarpley R, Suydam R (2004) Inferences from bowhead whale corpora data, age estimates, length at sexual maturity and ovulation rates. Paper SC/56/BRG8 presented to the IWC Scientific Committee, June 2004. Available from The International Whaling Commission, The Red House, 135 Station Road, Impington, Cambridge, Cambridgeshire CB24 9NP, United Kingdom.

George JC, Bada J, Zeh J, Scott L, Brown , O'Hara T, Suydam R (1999) Age and growth estimates of bowhead whales (*Balaena mysticetus*) via aspartic acid racemization. *Canadian Journal of Zoology,* 77, 571-80.

Givens GH., Huebinger RM, Patton JC, Postma LD, Lindsay M, Suydam RS, George JC, Matson CW, Bickham JW (2010) Population genetics of bowhead whales (*Balaena mysticetus*) from the western Arctic. Arctic 63, 1-12.

Harpending RC (1994) Signature of ancient population growth in a low-resolution mitochondrial DNA mismatch distribution. Human Biology, 66, 591-600.

Heide-Jørgensen MP, Laidre KL, Wiig Ø, Postma L, Dueck L, Bachmann L. 2010. Large-scale sexual segregation of bowhead whales. *Endangered Species Research*, 13, 73-78.

Hailer F, Helander B, Folkestad AO, et al. (2006) Bottlenecked but long-lived: high genetic diversity retained in white-tailedeagles upon recovery from population decline. *Biology Letters*, 22,316-319.

Heled J, Drummond AJ (2008) Bayesian inference of population size history from multiple loci. *BMC Evolutionary Biology*, 8, 289- 2008.

Hochberg Y (1988) A sharper Bonferroni procedure for multiple tests of sign. *Biometrika*, 75, 800-802.

Hoffman JI, Grant SM, Forcada J, Phillips CD (2011) Bayesian inference of a historical bottleneck in a heavily exploited marine mammal. *Molecular Ecology*, 20, 3989-4008.

Hudson RR (1990) Gene genealogies and the coalescent proces, pp. 1-44 in Oxford Surveys in Evolutionary Biology, edited by Futuyama, and J. D. Antonovics. Oxford University Press, New York.

Huebinger RM, Patton JC, George JC, Suydam RS, Louis Jr. EE, Bickham JW (2008) Characterization of twenty five microsatellite loci in bowhead whales (*Balaena mysticetus*). Molecular Ecology Resources 8, 612-615.

Jorde PE, Schweder T, Bickham JW, Givens GW, Suydam R, Hunter D, Stenseth NC (2007) Detecting genetic structure in migrating bowhead whales off the coast of Barrow, Alaska. Molecular Ecology 16,1993-2004.

Kimura M, Ohta T (1978) Stepwise mutation model and distribution of allelic frequencies in a finite population. *Proceedings of the National Academy of Sciences of the United States of America*, 75, 2868-2872.

Kimura M, Crow JF (1964) The number of alleles that can be maintained in a finite population. *Genetics*, 49, 725-738.

LeDuc RG, Martien KK, Morin PA, Hedrick N, Robertson KM, Taylor BL, Mugue NS, Borodin RG, Zelenina DA, Litovka D, George JC (2008) Mitochondrial genetic variation in bowhead whales in the western Arctic. *Journal of Cetacean Research and Management* 10, 93–97.

Lippé C, Dumont P, Bernatchez L (2006) High genetic diversity and no inbreeding in the endangered copper redhorse, Moxostoma hubbsi (Catostomidae, Pisces): the positive sides of a long generation time. *Molecular Ecology*, 15, 1769-1780.

Luikart G, Allendorf FW, Cornuet JM, Sherwin WB (1998) Distortion of allele frequency distributions provides a test for recent population bottlenecks. *Journal of Heredity*, 89, 238-247.

Nerini MK, Braham HW, Marquette WM, Rugh D. 1984. Life history of the bowhead whale, Balaena mysticetus (Mammalia: Cetacea). *Journal of Zoological Society of London*, 204, 443-468.

Phillips CD, Trujillo RG, Gelatt TS, Smolen MJ, Matson CW, Honeycutt RL, Patton JC Bickham JW (2009) Assessing substitution patterns, rates and homoplasy at HVRI of Steller sea lions, *Eumetopias jubatus*. *Molecular Ecology*, 18, 3379-3393.

Phillips CD, TS Gelatt, JC Patton, JW Bickham (2011) Phylogeography of Steller sea lions: relationships among climate change, effective population size, and genetic diversity. *Journal of Mammalogy*, 92, 1091-1104.

Parreira B, Trussart M, Sousa V, Hudson R, Chikhi L (2009) SPAms: A user-friendly software to simulate population genetics data under complex demographic models. *Molecular Ecology Resources*, 9, 749-753.

Piry S, Luikart G, Cornuet J-M (1999) BOTTLENECK: a computer program for detecting recent reductions in the effective population size using allele frequency data. *Journal of Heredity*, 90, 502-503.

Punt AE (2006) Assessing the Bering-Chukchi-Beaufort seas stock of bowhead whales using abundance data together with data on length or age. *Journal of Cetacean Research and Management*, 8, 127–137.

Rambaut A, Drummond AJ (2007) Tracer v1.4, Available from http://beast.bio.ed.ac.uk/Tracer

Raymond M, Rousset F (1995) Genepop (Version 1.2) - population genetics software for exact tests of ecumenicism. *Journal of Heredity*, 86, 248-249.

Rogers A (1995) Genetic evidence for a Pleistocene population explosion. *Evolution*, 49, 608-615.

Roman J, Palumbi S (2003) Whales before whaling in the north Atlantic. *Science*, 301, 508-510.

Rooney AP, Honeycutt RL, Davis SK, Derr J (1999) Evaluating a putative bottleneck in a population o bowhead whales from patterns of microsatellite diversity and genetic disequilibria. *Journal of Molecular Evolution*, 49, 682-690.

Rooney AP, Honeycutt R, Derr J (2001) Historical population size change of bowhead whales inferred from DNA sequence polymorphism data. *Evolution*, 55, 1678-1685.

Schneider S, Excoffier L (1999) Estimation of demographic parameters from the distribution of pairwise differences when the mutation rates vary among sites: application to human mitochondrial DNA. *Genetics*, 152:1079-1089.

Taylor B, LeDuc R, George JC, Suydam R, Moore S, Rugh D (2007) Synthesis of lines of evidence for population structure for bowhead whales in the Bering-Chukchi-Beaufort region. Paper SC/59/BRG35 presented to the IWC Scientific Committee, May 2007. Available from The International Whaling Commission, The Red House, 135 Station Road, Impington, Cambridge, Cambridgeshire CB24 9NP, United Kingdom.

Tamura K, Dudley J, Nei M, Kumar S (2007) MEGA4: Molecular Evolutionary Genetics Analysis (MEGA) software version 4.0. *Molecular Biology and Evolution*, 24, 1596-1599.

Tajima F (1989). Statistical method for testing the neutral mutation hypothesis by DNA polymorphism. *Genetics*, 123, 585-595.

Van Oosterhout C, Hutchinson WF, Wills DPM, Shipley P (2004) MICRO-CHECKER: software for identifying and correcting genotyping errors in microsatellite data. *Molecular Ecology Notes*, 4, 535-538.

Watterson G (1975) On the number of segregating sites in genetical models without recombination. *Theory in Population Biology*, 7, 256-276.

Figure Legends

Figure 1. Extended Bayesian skyline plot reconstructing N_{ef} over time. The grey area denotes the 95 highest posterior density for the estimates, the hashed line represents the mean, and the solid line represents the median estimates.

Figure 2. Plots of the posterior estimates of N_e values and μ under various prior assumptions on N_e. There were five N_e priors with associated time priors defined for analysis. The posterior estimates for these parameters are depicted in panels of the left column and are $N_{e(contempory)}$ = black line, $N_{e(bottleneck)}$ = long dashes, $N_{e(historicA)}$ = short dashes, and $N_{e(historicB)}$ = dotted. The panels of the right column depict the posterior estimates for average μ, and the organization of panels within rows corresponds to the prior bounds on N_e values that were assumed.

Figure 3. Box plots of heterozygosity values obtained through 1000 simulations for various combinations of contemporary N_e, historic N_e and, the timing of the population size change. The combination of parameters labelled 1-9 on the horizontal axis were 1 = 10,000, 50, 5; 2 = 10,000, 50, 50; 3 = 10,000, 50, 500; 4 = 10,000, 500, 5, 5 = 10,000, 500; 50; 6 = 10,000, 500, 500, 7 = 10,000, 1000, 5; 8 = 10,000, 1000, 50; and 9 = 10,000, 1000, 500. Simulation 7 represented the combination of parameter values most similar to that postulated for the BCB stock of bowhead whales. Mean heterozygosity for each set of simulations is listed above box plots and demarked with a solid dot within each box plot.

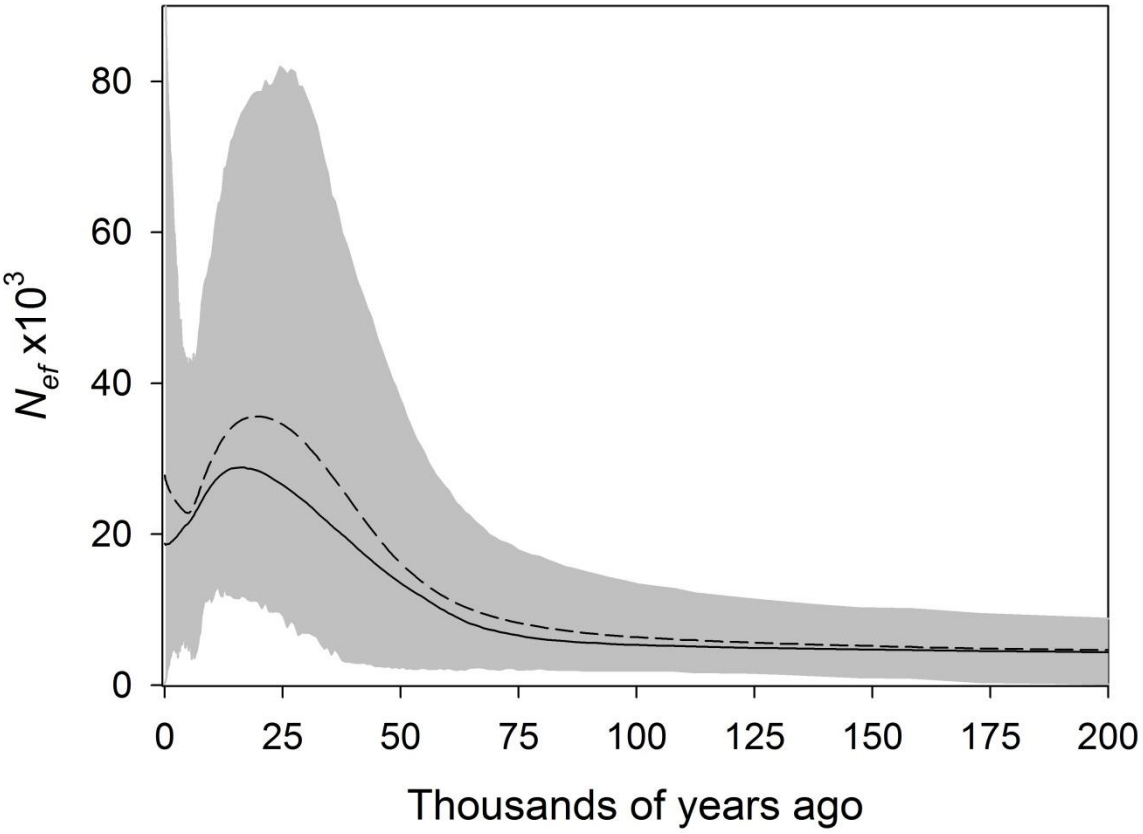
80
60
40
20
0
N_{ef} x10^3
0
25
50
75
100
125
150
175
200
Thousands of years ago

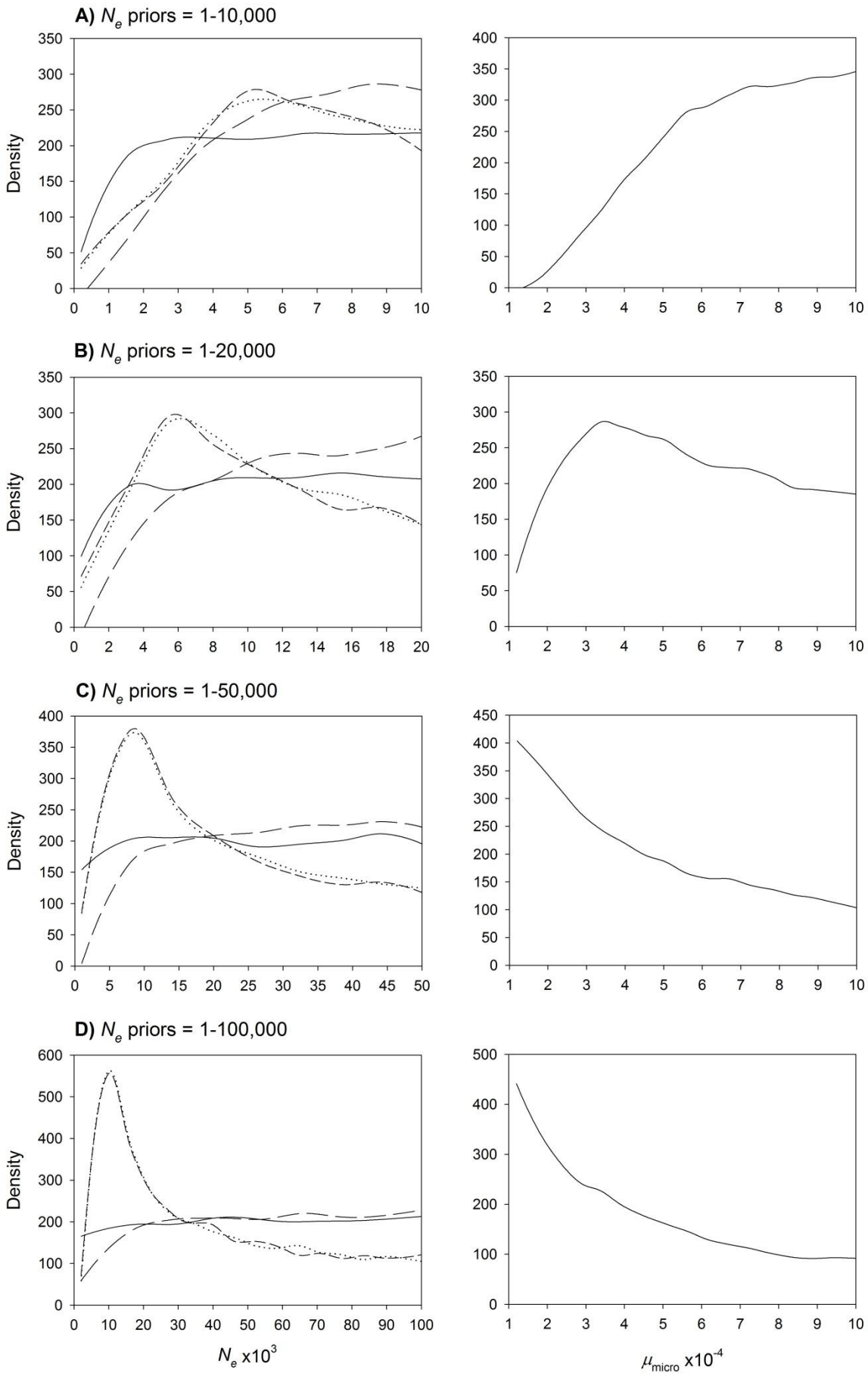
A) N_e priors = 1-10,000
B) N_e priors = 1-20,000
C) N_e priors = 1-50,000
D) N_e priors = 1-100,000
Density
N_e x10^3
μ_{micro} x10^{-4}

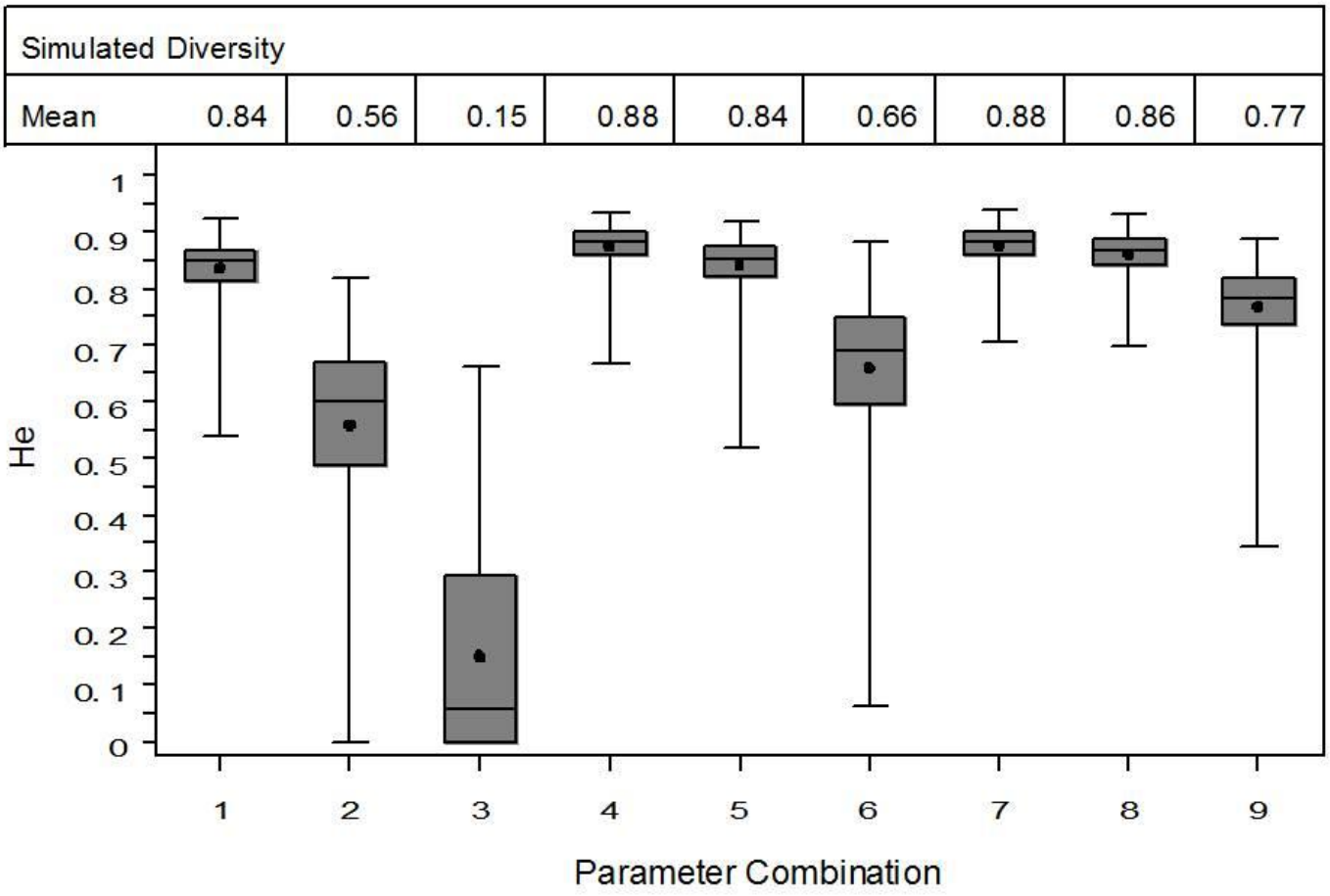
Simulated Diversity
Mean 0.84 0.56 0.15 0.88 0.84 0.66 0.88 0.86 0.77
He
1
0.9
0.8
0.7
0.6
0.5
0.4
0.3
0.2
0.1
0
1 2 3 4 5 6 7 8 9
Parameter Combination

Table 1. Summary of number of samples and sampling location for each population for microsatellites and mtDNA datasets.

Location	N microsatellites	N mtDNA
Barrow	260	137
Gambell	9	4
Savoonga	19	10
Kaktovik	16	9
Little Diomede	1	0
Nuiqsut	5	3
Point Hope	7	1
Wainwright	7	4
Total	324	168

Table 2. Details of the 22 microsatellite loci used in this study, including literature sources and polymorphism characteristics in 324 Bowhead whales.

Locus	Number of alleles	Observed heterozygosity (H_O)	Expected heterozygosity (H_E)	Hardy-Weinberg equilibrium probability	Probability of homozygote excess	Null allele frequency
Bmy1_1	10	0.822	0.812	0.159	0.550	-0.007
Bmy2_1	11	0.756	0.774	0.474	0.163	0.011
Bmy7_1	12	0.811	0.791	0.354	0.069	-0.014
Bmy8_1	16	0.783	0.800	0.504	0.095	0.010
Bmy10_1	22	0.890	0.926	0.386	**0.022**	0.019
Bmy11_1	14	0.870	0.878	0.274	0.485	0.004
Bmy12_1	27	0.930	0.922	0.653	0.227	-0.005
Bmy14_1	6	0.503	0.551	0.172	**0.015**	0.045
Bmy16_1	8	0.803	0.770	0.404	0.542	-0.022
Bmy18_1	17	0.881	0.902	0.693	0.099	0.011
Bmy19_1	16	0.843	0.867	0.282	0.052	0.013
Bmy26_1	22	0.895	0.925	0.385	**0.028**	0.016
Bmy33_1	13	0.798	0.807	**0.007**	0.508	0.005
Bmy36_1	28	0.938	0.939	0.787	0.506	0.000
Bmy41_1	22	0.896	0.905	0.088	**0.035**	0.004
Bmy42_1	11	0.722	0.781	0.397	**0.033**	0.039
Bmy49_1	24	0.895	0.892	0.098	0.390	-0.003
Bmy53_1	17	0.881	0.877	0.388	0.070	-0.003
Bmy54_1	8	0.680	0.707	0.237	**0.022**	0.019
Bmy55_1	6	0.682	0.710	**0.005**	**0.040**	0.019
Bmy57_1	9	0.566	0.602	**0.006**	**0.000**	0.029
Bmy58_1	27	0.929	0.926	**0.032**	0.450	-0.002
Average	15.7	0.808	0.821	–	–	

Table 3. The number of loci exhibiting heterozygosity excess and test probabilities obtained using a range of mutational models (see materials and methods for details) within the program BOTTLENECK [5]. Results are presented for separate analyses based on (a) the entire dataset; and (b) only the 18 loci that did not deviate significantly from HWE prior to correction for multiple tests. The mode test revealed normal L-shaped distributions under all of the scenarios tested. *P*-values significant at $\alpha < 0.05$ without correction for multiple statistical tests are highlighted in bold.

Mutational model	No. of loci with heterozygosity excess	No. of loci with heterozygosity deficiency	Sign test *P*-value	Standardized differences test *P*-value	Wilcoxon test *P*-value
All 22 loci:					
IAM	22	0	**<0.0001**	**<0.0001**	**<0.0001**
TPM70	18	4	**0.02129**	**0.01204**	**0.00528**
TPM90	12	10	0.43945	0.38970	0.87360
TPM95	8	14	**0.03066**	**0.02695**	0.13749
TPM99	4	16	**0.00279**	**<0.0001**	**0.00192**
SMM	5	17	**0.0006**	**<0.0001**	**0.0003**
18 loci in HWE:					
IAM	22	0	**<0.0001**	**<0.0001**	**<0.0001**
TPM70	18	4	**0.02129**	**0.01204**	**0.00528**
TPM90	12	10	0.43945	0.38970	0.87360
TPM95	8	14	**0.03066**	**0.02695**	0.13749
TPM99	4	16	**0.00279**	**<0.0001**	**0.00192**
SMM	5	17	**0.0006**	**<0.0001**	**0.0003**

Table 4. Point estimates and 95% credibility intervals for all N_e and μ obtained through simulations evoking different prior assumptions on N_e. * = because the posterior distributions for these parameters were mostly flat (Figure 2) point estimates for these parameters are weak estimates.

Parameter	mean	median	5%	95%
N_e (1-10,000)				
$N_{e(contemporary)}$ *	5.33×10^{-3}	5.37×10^{-3}	9.53×10^{-2}	9.54×10^{-3}
$N_{e(bottleneck)}$ *	6.22×10^{-3}	6.38×10^{-3}	2.13×10^{-3}	9.66×10^{-3}
$N_{e(historicA)}$	5.71×10^{-3}	5.77×10^{-3}	1.38×10^{-3}	9.50×10^{-3}
$N_{e(historicB)}$	5.74×10^{-3}	5.82×10^{-3}	1.45×10^{-3}	9.56×10^{-3}
M	6.80×10^{-4}	6.97×10^{-4}	3.24×10^{-4}	9.70×10^{-4}
N_e (1-20,000)				
$N_{e(contemporary)}$ *	1.04×10^{-4}	1.05×10^{-3}	1.41×10^{-3}	1.90×10^{-4}
$N_{e(bottleneck)}$ *	1.17×10^{-4}	1.20×10^{-3}	3.07×10^{-3}	1.93×10^{-4}
$N_{e(historicA)}$	9.60×10^{-3}	8.98×10^{-3}	1.70×10^{-3}	1.86×10^{-4}
$N_{e(historicB)}$	9.71×10^{-3}	9.12×10^{-3}	2.03×10^{-3}	1.87×10^{-4}
M	5.41×10^{-4}	5.24×10^{-4}	1.74×10^{-4}	9.46×10^{-4}
N_e (1-50,000)				
$N_{e(contemporary)}$ *	2.52×10^{-4}	2.50×10^{-4}	2.93×10^{-3}	4.74×10^{-4}
$N_{e(bottleneck)}$ *	2.74×10^{-4}	2.79×10^{-4}	5.50×10^{-3}	4.77×10^{-4}
$N_{e(historicA)}$	2.01×10^{-4}	1.69×10^{-4}	3.01×10^{-3}	4.57×10^{-4}
$N_{e(historicB)}$	2.04×10^{-4}	1.74×10^{-4}	3.01×10^{-3}	4.60×10^{-4}
M	4.10×10^{-4}	3.54×10^{-4}	7.29×10^{-5}	9.09×10^{-4}
N_e (1-100,000)				
$N_{e(contemporary)}$ *	5.10×10^{-4}	5.08×10^{-4}	5.73×10^{-3}	9.53×10^{-4}
$N_{e(bottleneck)}$ *	5.32×10^{-4}	5.39×10^{-4}	8.84×10^{-3}	9.55×10^{-4}
$N_{e(historicA)}$	3.62×10^{-4}	2.78×10^{-4}	3.66×10^{-3}	9.17×10^{-4}
$N_{e(historicB)}$	3.60×10^{-4}	2.79×10^{-4}	3.64×10^{-3}	9.08×10^{-4}
μ	3.51×10^{-4}	2.77×10^{-4}	3.80×10^{-5}	8.93×10^{-4}